



Article

Effective Adsorption of Phenoxyacetic Herbicides by Tomato Stem-Derived Activated Carbons

Krzysztof Kuśmierek ¹, Beata Doczekalska ^{2,*}, Maciej Sydor ³ and Andrzej Świątkowski ¹

- Institute of Chemistry, Faculty of Advanced Technologies and Chemistry, Military University of Technology, 00-908 Warsaw, Poland; krzysztof.kusmierek@wat.edu.pl (K.K.); a.swiatkowski@wp.pl (A.Ś.)
- Department of Chemical Wood Technology, Faculty of Forestry and Wood Technology, Poznań University of Life Sciences, 60-637 Poznan, Poland
- Department of Woodworking and Fundamentals of Machine Design, Faculty of Forestry and Wood Technology, Poznań University of Life Sciences, 60-637 Poznan, Poland; maciej.sydor@up.poznan.pl
- * Correspondence: beata.doczekalska@up.poznan.pl

Abstract: Six activated carbons from tomato (*Solanum lycopersicum* L.) stems (TS-AC) were synthesized by carbonization and chemical activation using potassium hydroxide (KOH) and sodium hydroxide (NaOH) at temperatures of 550, 650, and 750 °C. These TS-ACs were then evaluated as adsorbents to remove 2,4-dichlorophenoxyacetic acid (2,4-D) and 2-methyl-4-chlorophenoxyacetic acid (MCPA) from aqueous solutions. The adsorption kinetics of both herbicides followed the pseudo-second-order model, closely correlating with the mesopore volume of the TS-AC. The Langmuir isotherm accurately described the adsorption process for both 2,4-D and MCPA. The porous structure of TS-AC, characterized by micropore volume and specific surface area, significantly influenced the maximum adsorption capacities. The adsorption of both herbicides was pH dependent, but ionic strength had no significant effect. Regeneration testing, conducted over three cycles, showed less than a 15% reduction in herbicide adsorption capacity. This study demonstrates that agricultural waste, specifically tomato stems, can be effectively valorized by using simple activation techniques in TS-AC that are efficient adsorbents to remove organic pollutants, such as herbicides, from aqueous media.

Keywords: tomato stems; activated carbon; agricultural waste; chemical activation; surface chemistry; phenoxyacetic herbicides adsorption



Academic Editors: Luz Marina Ruíz and Miguel Ángel Gómez

Received: 14 May 2025 Revised: 6 June 2025 Accepted: 12 June 2025 Published: 17 June 2025

Citation: Kuśmierek, K.;
Doczekalska, B.; Sydor, M.;
Świątkowski, A. Effective Adsorption
of Phenoxyacetic Herbicides by
Tomato Stem-Derived Activated
Carbons. *Appl. Sci.* 2025, *15*, 6816.
https://doi.org/10.3390/app15126816

Copyright: © 2025 by the authors. Licensee MDPI, Basel, Switzerland. This article is an open access article distributed under the terms and conditions of the Creative Commons Attribution (CC BY) license (https://creativecommons.org/licenses/by/4.0/).

1. Introduction

Modern agriculture, forestry, and horticulture rely heavily on pesticides, with their use projected to escalate due to global food demand, the increased production of renewable energy and engineering materials, and the emergence of new pests and diseases. In 2022, according to the Food and Agriculture Organization, total pesticide use in agriculture reached 3.70 million tons [1]. This reflects a doubling of use since 1990, a 13% increase over the past decade, and a 4% increase from 2021. Compared to the 1990s, global pesticide use has increased by 121% for herbicides, 54% for fungicides and bactericides, and 48% for insecticides over the last decade [1]. The widespread use of these pollutants makes them one of the most serious environmental pollutants. They readily contaminate surface and groundwater through runoff and infiltration, negatively impacting aquatic ecosystems [2,3].

Herbicides currently constitute the largest group of pesticides in use, accounting for 56%, followed by fungicides at 25% and insecticides at 19% [1]. After glyphosate, the derivatives of phenoxyacetic acid, 2,4-dichlorophenoxyacetic acid (2,4-D), and 2-methyl-4-chlorophenoxyacetic acid (MCPA) represent the most commonly used herbicides [3]. These

two primary herbicides, designed to control broadleaf weeds in crops, pose a risk to aquatic environments due to their toxicity to living organisms [3,4]. Consequently, their degradation and removal from the ecosystem are a priority. Adsorption is a prevalent water purification technique, valued for its high efficiency, operational simplicity, and broad applicability [3,5–8]. Activated carbon (AC) is a commonly used adsorbent, particularly in granular form.

The high cost of commercially available activated carbon (AC) is primarily due to expensive production processes and non-renewable precursors such as coal, peat, and petroleum coke [9]. Consequently, researchers are investigating renewable, readily available, and inexpensive raw materials as alternative precursors for AC production. Low cost, renewability, and availability make biomass precursors particularly promising raw materials [3,10,11].

Recent research has explored numerous activated carbons, including those synthesized from wood, agricultural waste, and industrial biomass [10,11]. Plant-derived AC has been produced from various components, including peels, stems, shells, and other agricultural residues. These materials, primarily composed of cellulose biopolymers and other high-carbon-content polysaccharides, are suitable precursors for AC production. Lignocellulosic biomass offers an environmentally friendly and advantageous source for AC production. These precursors are diverse, readily available, and renewable, and their high reactivity simplifies the synthesis process [3,10]. In addition, it is also a reliable way to manage agricultural and household waste, which contributes to reducing disposal costs and negative environmental impacts.

Various parts of plants can be used to produce AC. This study explores the production of activated carbon from tomato stems (TS-AC) using a novel two-step process: pyrolysis followed by combined potassium hydroxide (KOH) and sodium hydroxide (NaOH) chemical activation. While previous research has examined TS-AC's properties, this work distinguishes itself through the specific activation methodology.

Recently, Zhi et al. [12] used the lotus petiole biomass in AC production, Bhungthong et al. [13] used palm shells as a precursor, Suhdi et al. [14] used rubber fruit shells, and Habeeb et al. [15] used the coconut shell. In all these works, KOH was used as the activation medium. The activating agent-to-precursor ratio often ranged from 1:1 to 4:1. In the work of Shao et al. [16], KOH precursor mass ratios of 2, 3, or 4 were selected.

Tiryaki et al. [17] investigated the production of AC from various natural biomass sources, including tomato stems and leaves, using phosphoric acid (H_3PO_4) chemical activation at 450 °C and an impregnation ratio of 1:2 (g/g). In particular, activated carbon derived from tomato stems (TS-AC) exhibited a significantly higher surface area (1248 m²/g) compared to that from tomato leaves (305 m²/g), highlighting the potential of tomato stems as a precursor.

Similarly, Yagmur [18] explored the impact of microwave radiation on AC production from various biomass raw materials, including tomato stems and leaves, using phosphoric acid (H_3PO_4) activation (2:1 precursor mass ratio). The duration of the microwave treatment (1–4 min at 900 W) strongly correlated with the type of precursor, microwave exposure, and AC properties. In particular, TS-AC demonstrated a significantly increased surface area after more long-lasting microwave exposure, peaking at 813.1 m²/g after 3 min before slightly decreasing to 705.4 m²/g at 4 min. This trend was observed alongside consistent pore size distribution across varying exposure times.

TS-AC was also produced from charred tomato stems through chemical activation with phosphoric acid (1:1 activating agent to precursor ratio) at 470 $^{\circ}$ C for 2 h [19]. A high specific Brunauer–Emmett–Teller (BET) surface area of 850 m²/g and a total pore volume of 0.5904 cm³/g enabled the synthesized TS-AC to adsorb phenol from water successfully.

Fu et al. [20] investigated the influence of the $FeCl_2$ impregnation ratio (from 1:1 to 3:1) and temperature (from 500 to 800 °C) on the porous structure of TS-AC. The study

revealed that increasing the FeCl₂-to-precursor ratio up to 2.5 enhanced both the specific surface area and micropore volume, with a subsequent decrease at higher impregnation ratios. Analogously, the TS-AC properties were enhanced with an increase in activation temperature up to 700 $^{\circ}$ C, followed by a deterioration at temperatures exceeding this value. Optimal activation conditions (2.5:1 impregnation ratio, 700 $^{\circ}$ C, 1 h process duration) resulted in TS-AC with a specific BET surface area of 971 m²/g and a micropore volume of 0.425 cm³/g, demonstrating the importance of controlled activation parameters.

Activators are critical in the activation process, with their reactivity varying significantly depending on biomass type and temperature [11]. Consequently, distinct activated carbons with varying physicochemical properties can be derived from the same precursor by altering synthesis conditions, particularly the activator. While acid and salt activation of tomato stems have been explored, to our knowledge, using a base as an activator remains unreported. This gap in research underscores the high relevance of this study.

Tomato stems are an easily accessible precursor source. In 2023, tomato cultivation in Poland accounted for 6150.63 hectares [21]. After harvesting tomatoes, the bushes are most often treated as waste. It is justified to confirm the concept of obtaining activated carbon from tomato stems by analyzing current research directions aimed at using various waste raw materials as precursors of carbon materials and considering the area of tomato cultivation. The research is part of activities aimed at developing and applying technologies for industrial purposes.

This study investigated the feasibility of producing activated carbons from tomato stem biomass through chemical activation using potassium hydroxide (KOH) and sodium hydroxide (NaOH). The research focused on analyzing the influence of the type of alkaline activating agent and activation temperature (550 °C, 650 °C, and 750 °C) on the porous structure, surface morphology, and chemical properties of the resulting carbon materials. The obtained TS-AC samples were subjected to physicochemical characterization and subsequently employed as adsorbents for the removal of organic contaminants—2,4-dichlorophenoxyacetic acid (2,4-D) and 2-methyl-4-chlorophenoxyacetic acid (MCPA)—from aqueous solutions. Furthermore, adsorption kinetics, equilibrium isotherms, and the effects of solution pH and ionic strength on adsorption efficiency were examined.

2. Experimental Section

2.1. Reagents and Raw Materials

2,4-Dichlorophenoxyacetic acid (2,4-D, >99%) was sourced from Acros Organics (Geel, Belgium) and 2-methyl-4-chlorophenoxyacetic acid (MCPA, >99%) from Sigma-Aldrich (St. Louis, MO, USA). The key physicochemical properties of these compounds are summarized in Table 1.

Table 1. Selected physicochemical properties of 2,4-dichlorophenoxyacetic acid (2,4-D) and 2-methyl-4-chlorophenoxyacetic acid (MCPA).

Adsorbate	CAS No.	Molecular Formula	Molecular Weight (g/mol)	Solubility in Water (g/L)	Acid Dissociation Constant, pK_a
2,4-D	94-75-7	CI CI OH	221.04	0.682	2.98
МСРА	94-74-6	CI CH ₃	200.62	0.825	3.14

Appl. Sci. **2025**, 15, 6816 4 of 21

Chempur (Piekary Śląskie, Poland) supplied the high-purity reagents (KOH, NaOH, HCl, NaHCO₃, Na₂CO₃, NaCl). Tomato stems for activated carbon production were sourced from greenhouse crops at horticultural farms in Greater Poland, west-central Poland.

2.2. Synthesis and Characterization of Activated Carbons from Tomato Stems (TS-AC)

Tomato stems were cleaned and dried to a constant weight at 105 °C. The dried stems underwent carbonization in a muffle furnace (Czylok, Jastrzębie-Zdrój, Poland) under an oxygen-free atmosphere with controlled process conditions. Carbonization was performed at 400 °C, 500 °C, and 600 °C, employing a heating rate of 3 °C/min and a 1 h dwell time at the target temperature. After completing the process, the chars were ground using an SM100 mill (Retsch GmbH, Haan, Germany) and then fractionated on sieves. A fraction of 0.5-1.0 mm of the chars prepared in this way was activated chemically using KOH or NaOH as activators (weight ratio of char to activator 1:4) in an argon atmosphere in a tube furnace (Czylok, Jastrzębie-Zdrój, Poland). The activation temperatures were 150 °C higher than the carbonization temperatures and were 550 °C, 650 °C, and 750 °C, respectively. Activation was performed for 15 min (time measured from the moment of reaching the target activation temperature), and the volume flow of argon was 20 dm³/h. The chemically activated carbon materials were extracted with 2% aqueous HCl for 8 h, then rinsed with distilled water until a neutral pH was achieved (approximately 12 h). The obtained material was then dried with a laboratory dryer at 105 °C to constant weight. TS-AC obtained in this way was abbreviated in the text by specifying the activating agent and the activation temperature in their name, e.g., AC-KOH-550 means TS-AC activated at 550 °C with potassium hydroxide, AC-NaOH-750 means TS-AC activated at 750 °C with sodium hydroxide, etc.

The yield was defined as the final weight of the product after the processing stages of activation, washing, and drying. The percent yield was calculated from Equation (1):

$$Yield = \frac{w_{AC}}{w_B} \cdot 100\% \tag{1}$$

where

 w_{AC} —dry activated carbon weight (g); w_{B} —dry carbonizate weight (g).

The surface chemistry of six activated carbons derived from tomato stems (TS-AC), produced by KOH and NaOH activation, was characterized. To determine the content of surface functional groups, the method of selective neutralization, employing standard solutions of NaOH, NaHCO $_3$, Na $_2$ CO $_3$, and HCl, was utilized according to the Boehm method [22]. The procedure was as follows: approximately 0.25 g of TS-AC was equilibrated with 25 mL of 0.01 mol/L NaOH or HCl solution by shaking for 24 h. Following degassing and filtration, the amount of bound neutralizing agent was determined by titration with 0.1 mol/L NaOH or HCl using the Tashiro index. Three replicate measurements were performed, and the average value was calculated.

Equation (2) was used to quantify the surface functional group content:

$$G_X = (V_0 - V_X) \cdot c \cdot \frac{25}{M_{AC}} \tag{2}$$

where

 G_x —content of selected oxygen surface groups (mmol/g);

 V_0 , V_x —amount of the HCl/NaOH solution used for titration of the supernatant sample (V_x) and the blank sample (V_0) (mL);

Appl. Sci. **2025**, 15, 6816 5 of 21

c—concentration of hydrochloric acid or sodium hydroxide (mol/L); M_{AC} —a mass of tomato stem-derived activated carbon (TS-AC) (g).

The point of zero charge (pH $_{pzc}$) of TS-AC was determined using the drift method. A series of Erlenmeyer flasks containing 20 mL of 0.01 mol/L NaCl solution was prepared, with initial pH values ranging from 2 to 12. These initial pH values were adjusted using 0.1 mol/L NaOH or HCl. Subsequently, 0.05 g of TS-AC was added to each flask, and the mixtures were shaken for 24 h. Following filtration, the final pH of each solution was measured. A plot of the final pH versus the initial pH was generated, and the pH $_{pzc}$ was determined as the intersection point of the resulting curve.

Thermogravimetric analysis (TGA) was performed using a thermal analysis test stand (STA 449 F5 Jupiter-QMS, NETZSCH-Gruppe, Burlington, MA, USA) to characterize the surface chemistry of the TS-AC further. Samples (15 \pm 1 mg) were heated from 25 °C to 950 °C at a rate of 10 °C/min under a helium flow of 25 cm³/min. Mass losses were quantified within the temperature ranges of 200–500 °C, 500–700 °C, and 700–950 °C for each TS-AC sample.

The TS-AC's surface morphology was examined using a scanning electron microscope (SEM) and Electron Dispersive Spectroscopy (EDS) (Zeiss EVO 10, Carl Zeiss Microscopy GmbH, Jena, Germany). Samples were mounted on carbon tape-coated SEM stubs and subsequently sputter-coated with gold (Quorum Q150R Plus, Quorum Technologies Ltd., Laughton, UK).

Nitrogen adsorption/desorption isotherms, measured at 77 K using an adsorption analyzer (ASAP 2020, Micromeritics Instrument Corp., Norcross, GA, USA), were employed to evaluate the porous structure parameters of the TS-AC. The carbon samples underwent degassing at 300 $^{\circ}$ C for 24 h before isotherm acquisition.

The iodine number to assess the adsorption capacity of selected TS-AC was determined (redox titration method) according to standardized test methods: ASTM D1510-24B [23] and ASTM D4607-14 [24]. When calculating the iodine value (IV), the following relationship was used:

$$IV = \frac{(V_0 - V_p)c_{tio} \cdot 126.92}{M_{AC}}$$
 (3)

where

 V_0 —the volume of sodium thiosulfate solution used in the blank (mL);

 V_p —the volume of sodium thiosulfate solution used in the actual determination (mL);

 c_{tio} —titer of sodium thiosulfate solution (mol/L);

*M*_{AC}—mass of the activated carbons (TS-AC) (g);

126.92—the mass of 0.5 moles of iodine (g).

2.3. Batch Adsorption Experiments

Adsorption experiments were conducted in Erlenmeyer flasks by adding 0.005 g of TS-AC to 20 mL of herbicide solutions of varying concentrations. The mixtures were shaken at 150 rpm and 23 °C. After a predetermined time, the solutions were filtered, and the filtrate was analyzed using a spectrophotometer (Cary 3E UV-Vis, Varian Medical Systems, Inc., Palo Alto, CA, USA). The equilibrium herbicide concentration (C_e , mmol/L) was used to calculate the adsorption efficiency ($Q_{\%}$) and adsorption capacity (Q_e , mmol/g) according to the following equations:

$$q_{\%} = \frac{(C_0 - C_e)}{C_0} \cdot 100\% \tag{4}$$

$$q_e = \frac{(C_0 - C_e)V}{m} \tag{5}$$

Appl. Sci. **2025**, 15, 6816 6 of 21

where C_0 and C_e are the initial and final (equilibrium) concentrations of 2,4-D or MCPA in solution (mmol/L), respectively; V is the volume of solution (L); and m is the mass of activated carbon (g).

In an analogous procedure, the amount of herbicide that was adsorbed after time t (q_t , mmol/g) was calculated:

$$q_t = \frac{(C_0 - C_t)V}{m} \tag{6}$$

where C_t (mmol/L) is the herbicide concentration at time t.

Kinetic studies were performed using an initial 1 mmol/L herbicide concentration. Adsorption isotherms were determined from a series of 2,4-D and MCPA solutions with different initial concentrations ranging from 0.3 to 1 mmol/L. Both kinetic and isotherm experiments were conducted at the solutions' natural pH (\sim 3.3). The influence of pH and ionic strength on herbicide adsorption was also investigated. Initial herbicide concentrations were maintained at 1 mmol/L for these experiments. Solutions were adjusted to pH values between 2.5 and 10 using 0.1 mol/L HCl or NaOH, monitored with an Elmetron CP-550 pH meter (Zabrze, Poland). Immediately following the pH adjustment, 0.005 g of activated carbon (AC) was added to each solution. NaCl was added to 20 mL of herbicide solutions to assess the effect of ionic strength to achieve final salt concentrations of 0.01, 0.1, and 0.5 mol/L. All adsorption experiments were duplicated, and the average value was used for subsequent calculations.

The regeneration of activated carbons studied was evaluated using methanol elution. The TS-AC was separated from the solution after adsorbing herbicides (1 mmol/L). Herbicide-loaded TS-AC (20 mg) was then agitated in 20 mL of methanol for 8 h using a laboratory shaker. Following filtration, the TS-AC was dried at 120 $^{\circ}$ C for 4 h and weighed. Subsequently, 20 mg of the regenerated TS-AC was added to 20 mL of 1 mmol/L 2,4-D or MCPA solution. This adsorption/desorption cycle was repeated three times, and the regeneration efficiency (R, %) was calculated using the following equation:

$$R = \frac{q_n}{q_0} \cdot 100\% \tag{7}$$

where q_0 is the initial adsorption capacity (mmol/g), and q_n is the reuse adsorption capacity (mmol/g) after the next cycle.

Herbicide concentrations in solutions were determined spectrophotometrically by measuring the absorbance at analytical wavelengths of 283 nm and 278 nm, corresponding to the absorption maximum of 2,4-D and MCPA, respectively. Calibration curves for their quantification, prepared in the range of 0.05 to 0.8 mmol/L, were linear ($R^2 \ge 0.996$) and described by the following equations: y = 1.448x + 0.021 (for 2,4-D) and y = 1.342x + 0.041 (for MCPA).

3. Results and Discussion

3.1. Properties of the Obtained Tomato Stem-Derived Activated Carbon (TS-AC)

Table 2 presents the surface chemistry parameters of the obtained TS-AC, including the contents of acidic and basic functional groups and point of zero charge values.

A comparison of KOH and NaOH activation reveals that increasing temperature reduces acidity and increases basic surface functional groups. However, KOH activation produced higher acidic and lower basic surface functional group content than NaOH.

Thermogravimetric analysis (TGA) results (Table 3), showing mass losses in the 200–500 °C, 500–700 °C, and 700–950 °C ranges, indicate the thermal decomposition of carboxyl, lactone, and hydroxyl groups, respectively [25]. These TGA findings corroborate the Boehm titration results (Table 2), which revealed a higher concentration of acidic oxygen

functional groups in KOH-activated carbons. Conversely, these carbons exhibited a lower concentration of basic functional groups.

Table 2. Surface characteristics of the tomato stem-derived activated carbon (TS-AC).

Activated Carbons	Total Acidic Groups (mmol/g)	Total Basic Groups (mmol/g)	Point of Zero Charge (pH _{pzc})
AC-KOH-550	3.03	1.66	6.65
AC-KOH-650	2.18	1.75	6.75
AC-KOH-750	1.23	3.28	7.15
AC-NaOH-550	1.84	2.02	7.00
AC-NaOH-650	1.23	4.18	7.20
AC-NaOH-750	0.82	4.92	7.25

Table 3. Mass loss results for tomato stem-derived activated carbon (TS-AC) samples.

TO A C	Mass Loss (%)							
TS-AC	200–500 °C	500–700 °C	700–950 °C	200–950 °C				
AC-KOH-550	3.6	5.6	5.9	15.1				
AC-KOH-650	2.7	4.3	4.8	11.8				
AC-KOH-750	1.7	2.6	3.2	7.5				
AC-NaOH-550	2.3	3.9	4.4	10.6				
AC-NaOH-650	1.8	3.0	3.4	8.2				
AC-NaOH-750	1.2	2.2	2.9	6.3				

An SEM-EDS analysis was performed to characterize the surface chemistry of the produced activated carbons. The determined percentage content of elements is presented in Table 4.

Table 4. Surface chemical composition of TS-AC samples determined by SEM-EDS.

TC ACCommis			Chemi	cal Comp	osition	(% wt.)		
TS-AC Sample	С	О	Ca	Mg	Al	Si	P	Zn
AC-KOH-550	84.3	12.7	1.7	0.4	0.1	0.1	0.4	0.2
AC-KOH-650	85.5	11.5	1.6	0.4	0.1	0.1	0.5	0.3
AC-KOH-750	88.6	9.2	1.2	0.4	0.1	0.1	0.4	-
AC-NaOH-550	83.0	13.5	2.2	0.4	0.1	0.1	0.4	0.2
AC-NaOH-650	86.8	10.1	1.7	0.4	0.1	0.3	0.3	0.2
AC-NaOH-750	88.3	9.8	1.0	0.3	0.1	0.1	0.2	0.1

It can be observed that with the increase in activation temperature, the carbon content increases, and the oxygen and calcium content decreases. This applies to both KOH and NaOH used as activating agents. Like other elements such as Mg, Al, Si, or P, their contents are small and practically do not change at different activation temperatures.

The SEM images of TS-AC reveal distinct morphological differences influenced by the choice of activating agent and the activation temperature. As illustrated in Figure 1, TS-AC samples activated with KOH and NaOH at 750 °C exhibit noticeable variations. For reference, the figure also includes an SEM image of the carbonizate obtained at 600 °C (biochar-600), which served as the precursor for both AC-KOH-750 and AC-NaOH-750 materials—notably, activation with NaOH results in the formation of finer particles, generally smaller than 10 μm .

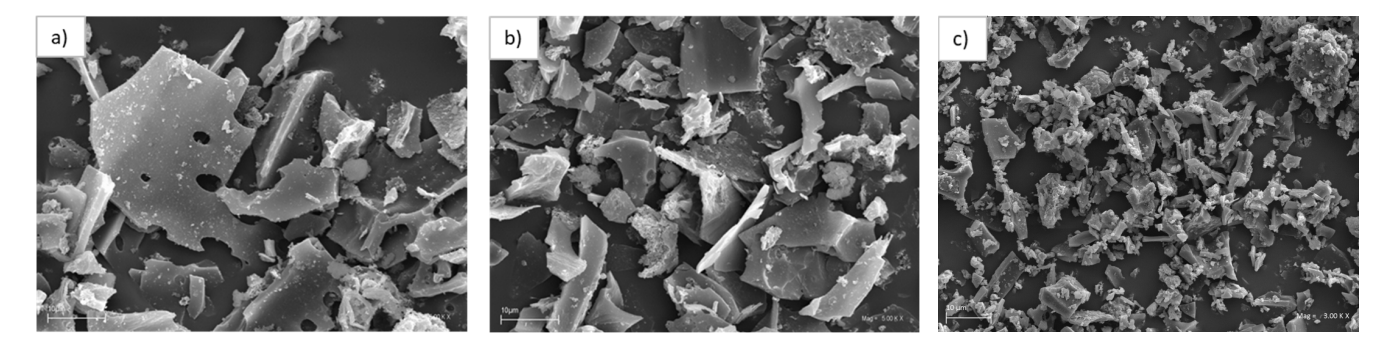


Figure 1. Example SEM images of activated carbons prepared from tomato stems (TS-AC): (a) AC-KOH-750; (b) AC-NaOH-750; (c) TS biochar-600.

Porous structure parameters of the TS-AC were determined from N_2 adsorption/desorption isotherms at 77 K (Figure 2).

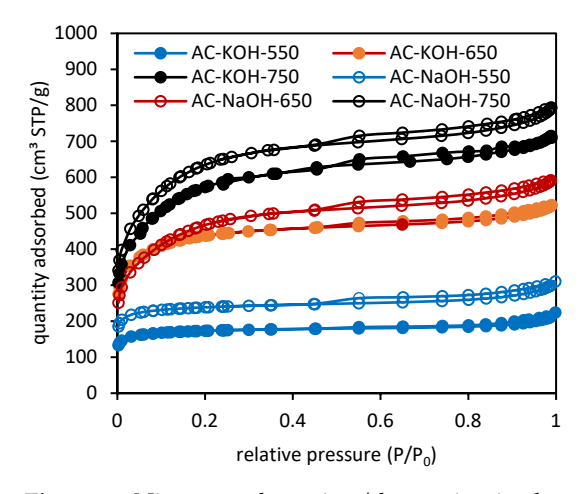


Figure 2. Nitrogen adsorption/desorption isotherms of activated carbon produced from tomato stems (TS-AC).

Specific surface areas ($S_{\rm BET}$, m²/g) were determined using the Brunauer–Emmett–Teller (BET) equation at relative pressure $p/p_o \approx 0.05$ –0.20. Total pore volumes ($V_{\rm t}$, cm³/g) were obtained from the adsorption isotherm at $p/p_o \approx 0.95$. Micropore volume ($V_{\rm mi}$, cm³/g) and mesopore volumes ($V_{\rm me}$, cm³/g) were calculated using the Barrett–Joyner–Halenda and t-plot methods. Average pore diameters $D_{\rm h}$ (nm) were calculated using the following formula: $4 \times V_{\rm t}/S_{\rm BET}$. The calculated porous structure parameter values are presented in Table 5.

Table 5. The textural characteristics and yield of the activated carbon from tomato stems (TS-AC).

TS-AC	BET Surface Areas, S _{BET} (m ² /g)	Micropore Volume, V _{mi} (cm ³ /g)	Total Pore Volume, V _t (cm ³ /g)	Mesopore Volume, $V_{\rm me}$ (cm 3 /g)	V _{mi} /V _t (%)	Average Pore Diameters, $D_{\rm h}$ (nm)	Iodine Number (mg/g)	Yield (%)
AC-KOH-550	575	0.268	0.323	0.055	82.97	2.25	940	56.4
AC-KOH-650	1445	0.677	0.798	0.121	84.84	2.21	1260	45.9
AC-KOH-750	1810	0.788	1.082	0.294	72.83	2.39	1290	39.8
AC-NaOH-550	790	0.369	0.455	0.086	81.10	2.30	1060	42.5
AC-NaOH-650	1565	0.723	0.903	0.180	80.07	2.31	1280	30.6
AC-NaOH-750	2085	0.928	1.211	0.283	76.63	2.32	1320	22.2

A direct correlation was observed between activation temperature and $S_{\rm BET}$, $V_{\rm t}$, and $V_{\rm mi}$ values. NaOH activation produced superior porous structure parameters compared to KOH activation at equivalent temperatures. This trend was further validated by iodine number values, which confirmed the observed pattern while elevated relative to BET surface areas from nitrogen adsorption/desorption isotherms.

Appl. Sci. 2025, 15, 6816 9 of 21

Another dependence exists between $V_{\rm mi}/V_{\rm t}$ and $D_{\rm h}$. The increase in $V_{\rm mi}/V_{\rm t}$ results in a decrease in D_h . The lowest V_{mi}/V_t values were observed for AC KOH-750 and NaOH-750. Activated carbon (TS-AC) synthesized at 650 °C and 750 °C has significantly higher BET surface areas (S_{BET}) than those obtained by other authors using other activators. For example, the BET surface areas of the activated carbons prepared from tomato stems (TS-AC) by chemical activation using phosphoric acid were $1248 \text{ m}^2/\text{g} [17]$, $850 \text{ m}^2/\text{g} [19]$, and 813 m²/g [18]. In contrast, the BET surface area of the TS-AC prepared by activation with FeCl₂ was 971 m²/g [20]. In the case of chemical activation, the raw lignocellulosic precursor is usually impregnated directly with an activator. The ratio of the chemical activator to precursor mass, along with the process time and temperature, is essential, but perhaps the most critical factor is the type of activator used [10,11]. Activators of different types (acids, alkalis, or salts) can interact differently with the lignocellulosic precursor, determining the activated carbon production process. Phosphoric acid exhibits a dual action: it degrades cellulose and hemicellulose polymers in biomass and simultaneously reacts with and dissolves lignin and cellulose. Salts, e.g., ZnCl₂ or FeCl₂, as activating agents, usually act as dehydrating agents after impregnation of the biomass, causing hydrolysis reactions. The alkaline activators react with the lignin and dissolve the ether bonds and hydroxyl groups, resulting in the delignification of the precursor [11].

An increase in activation temperature from 550 °C to 750 °C resulted in reduced process yields (Table 5). Notably, higher yields were observed when potassium hydroxide was used as the activating agent.

The results suggest that the alkali interaction with the tomato stems is the most beneficial and results in activated carbons with the highest BET surface areas (S_{BET}).

3.2. Adsorption Study

3.2.1. Adsorption Kinetics

Figure 3 depicts the adsorption kinetics of 2,4-D and MCPA on tomato stem-derived activated carbon (TS-AC) as a function of time, demonstrating the rapid adsorption in the initial stage (within the first few minutes) and then slowing down, reaching equilibrium after about 60 min.

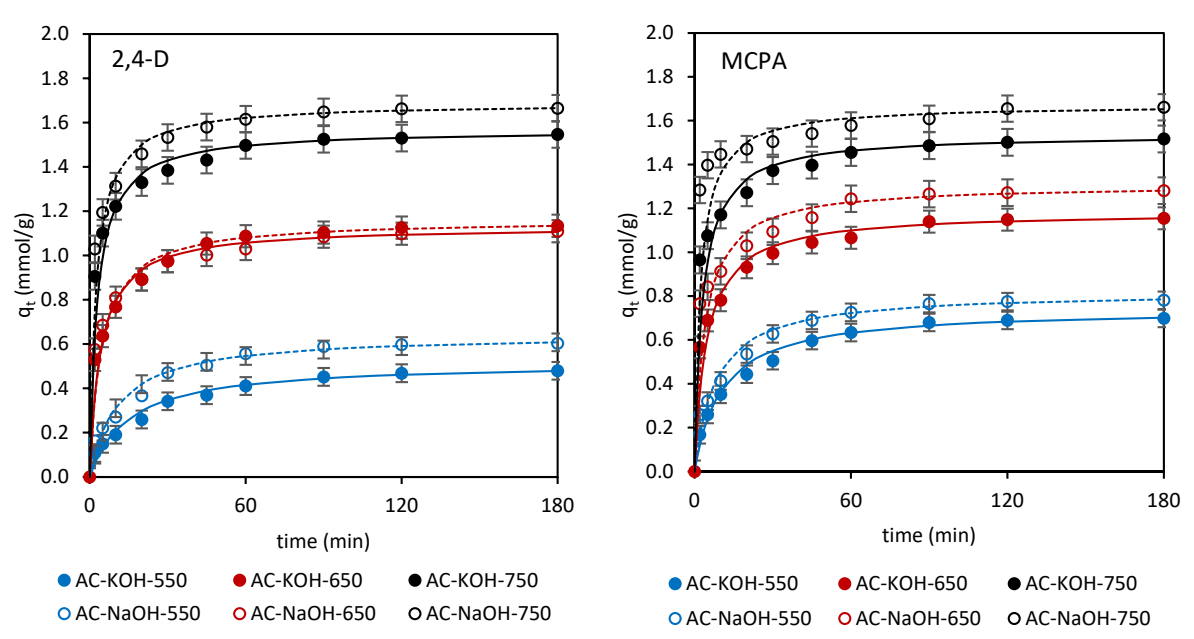


Figure 3. Adsorption kinetics of 2,4-dichlorophenoxyacetic acid (2,4-D) and 2-methyl-4-chlorophenoxyacetic acid (MCPA) on tomato stem-derived activated carbon (TS-AC) (lines mean the fitting of the pseudo-second-order (PSO) kinetic model). Conditions: adsorbate initial concentration = 1 mmol/L, adsorbent dosage = 0.25 g/L, pH = original (~3.3), temperature = $23 \, ^{\circ}\text{C}$.

The correlations obtained clearly show that TS-AC prepared at the same activation temperature has similar adsorption properties (the plot curves are similar). However, two kinetic models, pseudo-first-order (PFO) and pseudo-second-order (PSO), were used to compare the adsorption kinetics reliably. The following dependence expresses the PFO model proposed by Sten Lagergren [26]:

$$\log (q_{\rm e} - q_{\rm t}) = \log q_{\rm e} - \frac{k_1}{2.303}t \tag{8}$$

where k_1 is the pseudo-first-order adsorption rate constant (1/min).

The rate constant of the PFO model was determined from the slope and intercept obtained for the linear function $log(q_e - q_t) = f(t)$.

The pseudo-second-order kinetic model, proposed by Ho and McKay [27], can be represented as follows:

$$\frac{t}{q_{\rm t}} = \frac{1}{k_2 q_{\rm e}^2} + \frac{1}{q_{\rm e}} t \tag{9}$$

where k_2 is the pseudo-second-order adsorption rate constant (g/mmol·min) determined from the slope and intercept obtained for the linear relationship $t/q_t = f(t)$.

The determination coefficients (R^2) and chi-square (χ^2) values were used to assess the kinetic model's fit to the experimental data. R^2 values were calculated using the following formula:

$$R^{2} = \frac{\sum_{i=1}^{n} (q_{e(\text{cal})} - \overline{q_{e(\text{exp})}})^{2}}{\sum_{i=1}^{n} (q_{e(\text{cal})} - \overline{q_{e(\text{exp})}})^{2} + \sum_{i=1}^{n} (q_{e(\text{cal})} - q_{e(\text{exp})})^{2}}$$
(10)

where $q_{e(exp)}$ and $q_{e(cal)}$ are the adsorption capacities (mmol/g) obtained experimentally and calculated from the kinetic model (Equations (4) and (5)), respectively.

The χ^2 value was calculated using the following equation:

$$\chi^{2} = \sum_{i=1}^{n} \frac{\left(q_{e(\exp)} - q_{e(\text{cal})}\right)^{2}}{q_{e(\text{cal})}}$$
(11)

МСРА

A better fit of the model is indicated by higher R^2 (closer to 1) and lower values of χ^2 . Kinetic modeling data for the adsorption of the herbicides on AC produced from tomato stems are listed in Table 6.

Table 6. Kinetic parameters for 4-dichlorophenoxyacetic acid (2,4-D) and 2-methyl-4-chlorophenoxyacetic acid (MCPA) adsorption on tomato stem activated carbon (TS-AC).

2 4-D

		2,4-1)			MCPA					
TS-AC		Pseudo-First-Order (PFO) Kinetic Model								
13-AC	(1/min)	R^2	χ^2	k ₁ (1/min)	R^2	χ^2				
AC-KOH-550	0.0299	0.991	0.185	0.0356	0.981	0.045				
AC-KOH-650	0.0368	0.958	0.522	0.0396	0.971	0.089				
AC-KOH-750	0.0342	0.911	0.711	0.0472	0.941	0.258				
AC-NaOH-550	0.0502	0.955	0.369	0.0391	0.990	0.029				
AC-NaOH-650	0.0472	0.927	0.412	0.0386	0.953	0.337				
AC-NaOH-750	0.0504	0.978	0.089	0.0327	0.901	0.679				
		Pseudo-second-order (PSO) kinetic model								
	k ₂ (g/mmol·min)	R^2	χ^2	k ₂ (g/mmol·min)	R^2	χ^2				
AC-KOH-550	0.130	0.997	0.023	0.128	0.998	0.029				
AC-KOH-650	0.187	0.999	0.011	0.181	0.999	0.017				
AC-KO11-050										
AC-KOH-750	0.235	0.999	0.019	0.259	0.999	0.014				
		0.999 0.998	0.019 0.038	0.259 0.151	0.999 0.999	0.014 0.015				
AC-KOH-750	0.235									

The q_e ($q_{e(cal)}$) values from the PSO model were closer to $q_{e(exp)}$ than those from the PFO model, which also exhibited higher R^2 and lower χ^2 values, showing a better fit. This is illustrated in Figure 4.

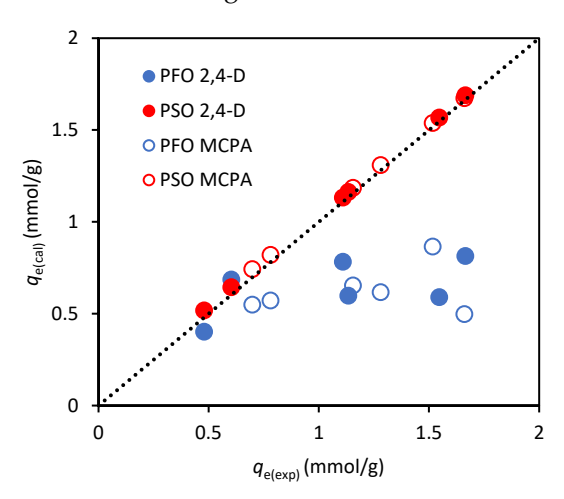


Figure 4. The correlation between the experimentally determined ($q_{e(exp)}$) and model-calculated ($q_{e(cal)}$) amounts of the adsorbed herbicide, using the pseudo-first-order (PFO, blue circles) and pseudo-second-order (PSO, red circles) kinetic models.

Based on these findings, the PSO kinetic model accurately describes the adsorption of 2,4-D and MCPA on TS-AC. This aligns with previous research, as reviews [3,7,8,28] indicate that the PSO model is commonly the most suitable for phenoxyacetic herbicide adsorption onto various adsorbents.

As shown by the very similar k_2 values, both herbicides were adsorbed on individual AC at more or less the same rate. However, the disparities become more apparent when adsorbents are compared against each other rather than the adsorbates. The k₂ values obtained for both herbicides increase in order: AC-KOH-550 < AC-NaOH-550 < AC-KOH-650 < AC-NaOH-650 < AC-NaOH-750 < AC-KOH-750. Thus, 2,4-D and MCPA adsorbed rapidly on AC-KOH-750 and most slowly on AC-KOH-550. This observed sequence seems closely related to the porous structure of these activated carbons, as shown in Table 4. While the adsorption capacity of adsorbents is primarily determined by micropore volume and BET surface area, the adsorption rate is influenced mainly by mesopore volume. Mesopores (2-50 nm diameter) serve as transport pathways, facilitating adsorbate molecule diffusion into the adsorbent particle and ultimately to the micropores, where adsorption occurs via surface interaction. Consequently, a greater mesopore volume generally correlates with a faster rate of adsorbate uptake from the solution. Both 2,4-D and MCPA adsorbed most slowly on AC-KOH-550, which has the smallest mesoporous structure ($V_{\text{me}} = 0.055 \text{ cm}^3/\text{g}$). On the other hand, adsorption occurred most rapidly on AC-KOH-750, the adsorbent with the largest mesopore volume ($V_{\rm me} = 0.337 \, {\rm cm}^3/{\rm g}$). Thus, individual ACs' observed adsorption rate characteristic is closely correlated with their mesoporous structure (mesopore volume).

Although the PSO kinetic model describes the adsorption kinetics well, it does not explain the adsorption mechanism. Therefore, a diffusion model was also used to describe the kinetics [29]. This is the Weber–Morris model [30], also known as the intra-particle diffusion model [31], which is expressed by the following formula:

$$q_t = k_i t^{0.5} + C_i (12)$$

where k_i is the intra-particle diffusion rate constant (mmol/g·min^{-0.5}) and C_i is the thickness of the boundary layer.

The Weber–Morris model makes it possible to determine which stage of the adsorption process determines the rate of the overall process. It is usually film diffusion, pore (intraparticle) diffusion, or a combination of both [29].

According to the assumptions of this model, the following variants are possible.

- The plot of $q_t = f(t^{0.5})$ is a straight line over the whole range—the adsorption rate is controlled by only one step (film diffusion or intra-particle diffusion).
- The plot of $q_t = f(t^{0.5})$ is not linear over the whole range (broken line)—the adsorption is more complex, and both stages, film diffusion and intra-particle diffusion, control its rate.
- The plot of $q_t = f(t^{0.5})$ passes through the origin (intercept = 0)—intra-particle diffusion is the primary rate-limiting step in adsorption.
- The plot of $q_t = f(t^{0.5})$ does not pass through the origin (intercept $\neq 0$)—pore diffusion plays a secondary role, and the rate of the overall adsorption process is controlled by film diffusion.

Figure 5 shows the Weber–Morris model results. The non-linear plots of q_t vs. $t^{0.5}$, not passing through the origin, suggest multiple rate-controlling processes with dominant film diffusion.

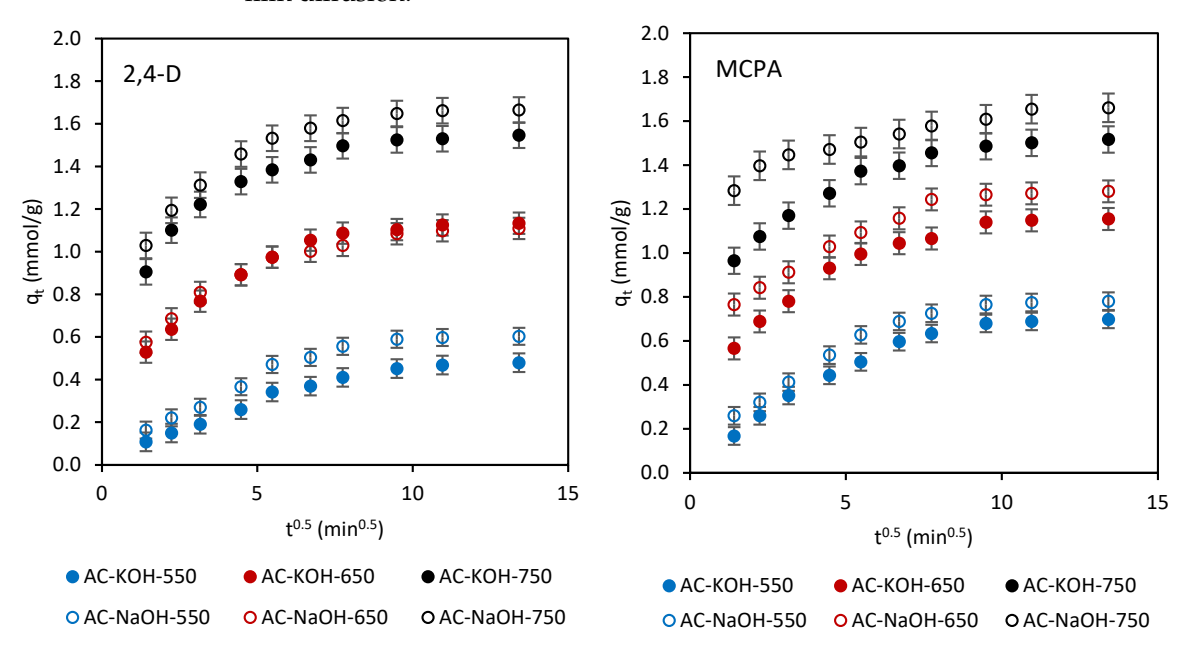


Figure 5. The Weber–Morris diffusion model plots for adsorption of 2,4-D and MCPA on tomato stem activated carbon (TS-AC).

3.2.2. Adsorption Isotherms

The correlations between the adsorbed amount (q_e) and the adsorbate concentration at equilibrium (C_e) are shown in Figure 6.

Langmuir [32] and Freundlich [33] models, the two most commonly used theoretical approaches [34], were applied to describe the experimental adsorption isotherms. The equation of the Langmuir isotherm has the following form:

$$\frac{C_{\rm e}}{q_{\rm e}} = \frac{1}{q_{\rm m}} C_{\rm e} + \frac{1}{q_{\rm m} K_{\rm L}} \tag{13}$$

where $q_{\rm m}$ is Langmuir's maximum adsorption capacity (mmol/g) and $K_{\rm L}$ is the Langmuir isotherm constant (L/mmol).

These isotherm parameters were calculated from the slope and intercept obtained for the linear relationship of C_e/q_e vs. C_e .

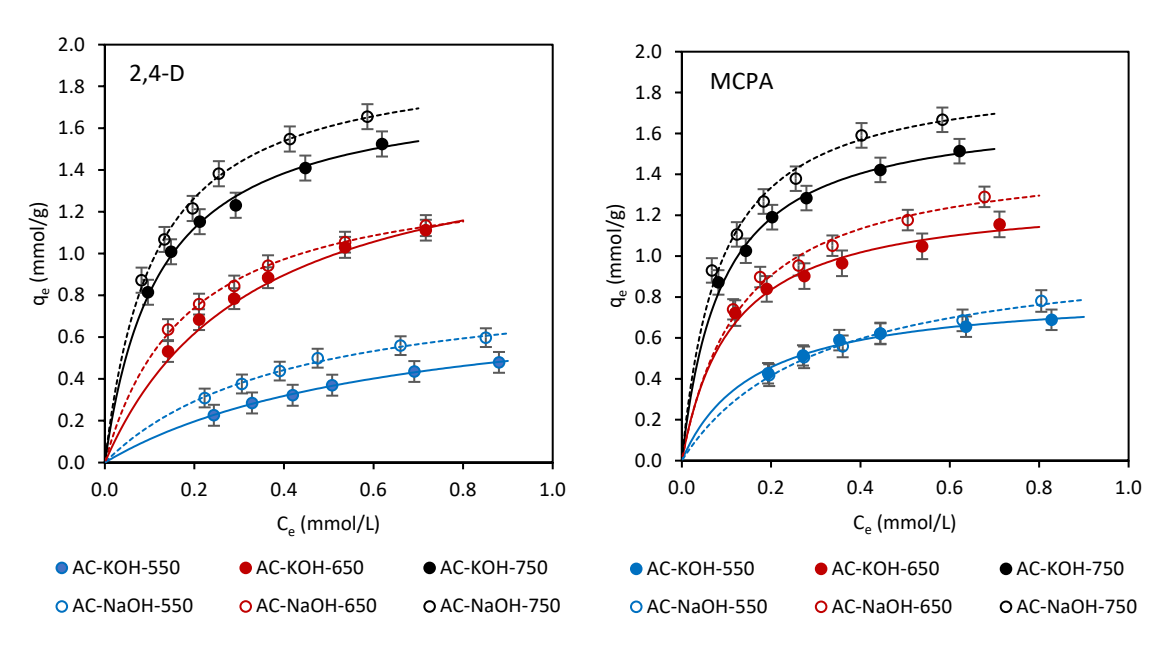


Figure 6. Adsorption isotherms of 2,4-D and MCPA on tomato stem-derived activated carbon (TS-AC) (line: fitting of Langmuir isotherm) (experimental conditions: herbicides initial concentrations from 0.3 to 1 mmol/L, adsorbent dosage = 0.25 g/L, pH = original (~3.3), temperature = $23 \,^{\circ}\text{C}$).

The Freundlich isotherm equation has the following form:

$$\ln q_e = \ln K_{\rm F} + \frac{1}{\rm n} \ln C_{\rm e} \tag{14}$$

where K_F is the Freundlich isotherm constant related to adsorption capacity (mmol/g) $(L/mmol)^{1/n}$ and n is the Freundlich isotherm constant (dimensionless).

The $K_{\rm F}$ and 1/n values were calculated from the slope and intercept obtained for the linear plot $\ln q_{\rm e} = f(\ln C_{\rm e})$.

As in the case of the kinetic models, the evaluation of the fit of the experimental data to the theoretical models was based on the analysis of the R^2 and χ^2 values obtained. Lower χ^2 values and R^2 values closer to unity indicated a better model fit. The parameters of the Langmuir and Freundlich isotherms and the R^2 and χ^2 values describing the adsorption of 2,4-D and MCPA on activated carbons derived from tomato stem (TS-AC) are listed in Table 7.

Table 7. Langmuir and Freundlich isotherm parameters for the adsorption of 2,4-dichlorophenoxyacetic acid (2,4-D) and 2-methyl-4-chlorophenoxyacetic acid (MCPA) on activated carbon derived from tomato stems (TS-AC).

		2,4	-D			M	CPA			
TS-AC		Langmuir Isotherm Model								
	$q_{ m m}$	$K_{\rm L}$	R^2	χ^2	q_{m}	K_{L}	R^2	χ^2		
AC-KOH-550	0.840	1.530	0.996	0.0013	0.830	6.136	0.996	0.0024		
AC-KOH-650	1.417	5.468	0.999	0.0012	1.302	8.972	0.995	0.0068		
AC-KOH-750	1.806	8.201	0.998	0.0025	1.721	11.08	0.999	0.0045		
AC-NaOH-550	0.904	2.398	0.993	0.0011	1.056	3.244	0.993	0.0016		
AC-NaOH-650	1.637	3.030	0.997	0.0012	1.513	7.466	0.994	0.0062		
AC-NaOH-750	1.960	9.129	0.999	0.0029	1.902	11.78	0.998	0.0034		
			Fre	eundlich is	otherm n	nodel				
	K _F	1/n	R^2	χ^2	K_{F}	1/n	R^2	χ^2		
AC-KOH-550	0.534	0.584	0.990	0.0033	0.766	0.314	0.914	0.0079		
AC-KOH-650	1.311	0.357	0.990	0.0281	1.247	0.251	0.992	0.0091		
AC-KOH-750	1.831	0.326	0.979	0.0058	1.778	0.276	0.982	0.0075		
AC-NaOH-550	0.682	0.501	0.972	0.0063	0.857	0.424	0.990	0.0049		
AC-NaOH-650	1.377	0.497	0.973	0.0088	1.451	0.300	0.987	0.0090		
AC-NaOH-750	2.057	0.329	0.980	0.0079	2.002	0.280	0.990	0.0071		

 $q_{\rm m}$ (mmol/g); $K_{\rm L}$ (L/mmol); $K_{\rm F}$ ((mmol/g)(L/mmol)^{1/n}).

The results indicate that both the Langmuir and the Freundlich models effectively describe the experimental data. However, the Langmuir isotherm model exhibited marginally higher R^2 values and marginally lower χ^2 values. This suggests that the adsorption of both herbicides on activated carbon from tomato stems (TS-AC) follows the Langmuir model rather than the Freundlich model. This suggests that the adsorption process most likely forms a monomolecular adsorbate layer on the TS-AC surface, implying a finite number of energetically homogeneous adsorption sites and negligible interactions between adsorbed molecules.

The Langmuir model also provides insights into the nature and favorability of the adsorption process. The separation factor (R_L), which indicates adsorption favorability, can be calculated from the Langmuir constant (K_L) using the following equation [34]:

$$R_L = \frac{1}{1 + K_L C_0} \tag{15}$$

Table 8 presents the calculated $R_{\rm L}$ values (minimum and maximum values for each AC). These values, ranging between zero and one (0 < $R_{\rm L}$ < 1), confirm the favorable nature of the adsorption process. In another situation, if the value of $R_{\rm L}$ were equal to 0 or 1, the adsorption would be irreversible or linear, respectively. Conversely, a value of $R_{\rm L}$ greater than 1 would indicate the unfavorable nature of the adsorption [34].

Table 8. The Gibbs free energy change (ΔG°) and separation factors ($R_{\rm L}$) associated with the adsorption of 2,4-dichlorophenoxyacetic acid (2,4-D) and 2-methyl-4-chlorophenoxyacetic acid (MCPA) onto tomato stem-derived activated carbon (TS-AC).

		2,4-D			MCPA			
TS-AC	ΔG° Separation		Factor (R _L)	ΔG°	Separation	Separation Factor (R _L)		
	(kJ/mol)	Min.	Max.	(kJ/mol)	Min.	Max.		
AC-KOH-550	-27.9	0.395	0.685	-31.4	0.140	0.352		
AC-KOH-650	-31.1	0.154	0.379	-32.3	0.101	0.271		
AC-KOH-750	-32.1	0.109	0.289	-32.8	0.083	0.231		
AC-NaOH-550	-29.1	0.294	0.581	-29.8	0.236	0.506		
AC-NaOH-650	-29.6	0.248	0.523	-31.8	0.118	0.308		
AC-NaOH-750	-32.3	0.098	0.267	-33.0	0.078	0.221		

The Freundlich isotherm constant, 1/n, substantiates the conclusions regarding the favorability of adsorption. Values of 1/n exceeding or equaling 1 ($1/n \ge 1$) indicate unfavorable or irreversible adsorption processes, respectively. Conversely, a 1/n value within the interval of 0 to 1 (0 < 1/n < 1) is characteristic of favorable adsorption [34]. As shown in Table 6, the 1/n values for all activated carbons ranged from 0.326 to 0.501 for 2,4-D and from 0.251 to 0.424 for MCPA, indicating a favorable adsorption process.

The Langmuir constant K_L can be used to calculate the Gibbs free energy change (ΔG°) [35] for adsorption [36]. The ΔG° was calculated using the following equation:

$$\Delta G^{\circ} = -RT \ln(55.5K_L) \tag{16}$$

where R is the universal gas constant (8.314 J/mol·K) and T is the temperature in Kelvin.

This parameter quantifies the spontaneity and feasibility of the adsorption process. Negative ΔG° values indicate a spontaneous reaction. The calculated ΔG° values are presented in Table 8, all of which are negative, confirming the spontaneous nature of the adsorption.

The analysis of the $q_{\rm m}$ and $K_{\rm F}$ values shown in Table 7 shows that both herbicides were better adsorbed onto TS-AC activated with NaOH than with KOH at the same temperatures. AC-KOH-550 was the weakest adsorbent, while AC-NaOH-750 showed the highest adsorption capacity. This trend (AC-KOH-550 < AC-NaOH-550 < AC-KOH-

650 < AC-NaOH-650 < AC-KOH-750 < AC-NaOH-750) appears to correlate strongly with the porous structure of the TS-AC. In addition to the surface chemistry, textural properties, including micropore volume and specific surface area, significantly influence the adsorption characteristics of TS-AC. Generally, the adsorption capacity of an adsorbent is directly proportional to its micropore volume ($V_{\rm mi}$) and specific surface area ($S_{\rm BET}$), owing to the increased availability of active sites for adsorbate molecule interaction. Thus, the lowest adsorption capacity of AC-KOH-550 results from its most poorly developed porous structure ($V_{\rm mi} = 0.268~{\rm cm}^3/{\rm g}$, $S_{\rm BET} = 575~{\rm m}^2/{\rm g}$). AC-NaOH-750 appeared to be the most effective adsorbent, having the highest micropore volume and specific surface area ($V_{\rm mi} = 0.928~{\rm cm}^3/{\rm g}$ and $S_{\rm BET} = 2085~{\rm m}^2/{\rm g}$, respectively). The adsorption properties of the other ACs are also correlated with their microporous structure and BET surface area. This strong correlation observed for both herbicides suggests that the textural properties of the tomato stem-derived activated carbon (TS-AC) have a more significant influence on herbicide adsorption than their surface chemistry.

In our earlier works [37,38], it was also found that the effect of activated carbon surface chemistry on the sorption capacity of chloroorganic compounds is smaller than the effect of porosity development. This was demonstrated in the granular activated carbon samples with very little differentiation of porous structure parameters and enormously different surface chemistry. In the case of activated carbon samples with enormously different porous structure parameters and almost identical surface chemistry, a correlation was found between the adsorption capacity of chloroorganic compounds (e.g., chlorophenol) and their BET surface area and micropore volume [39].

A consistent trend was observed across all six TS-AC: 2,4-D exhibited a slightly higher adsorption tendency than MCPA. This finding is supported by the literature, which has documented similar results for these herbicides on various adsorbents, including switchgrass biochar [40], Filtrasorb 300 activated carbon [41], AC from pistachio shells prepared via physical activation [42], or some carbon blacks [43]. However, this is not a definite trend, as there are just as many reports of better adsorption of MCPA compared to 2,4-D [44–49]. Therefore, the observed variability in the relative adsorption of 2,4-D and MCPA is more accurately described due to the distinct physicochemical attributes inherent to each adsorbent.

These properties influence the mechanism of herbicide molecule attachment to the adsorbent surface. The adsorption mechanism of phenoxyacetic herbicides, focusing on 2,4-D, has been thoroughly investigated and summarized in recent reviews [3,7,8]. The adsorption of 2,4-D on activated carbons results from hydrophobic and π - π interactions, attractive and/or repulsive electrostatic interactions, and hydrogen bonding interactions [3,7,8]. As anticipated, the adsorption of 2,4-D on TS-AC proceeded via these mechanisms. Given the structural similarity of MCPA to 2,4-D, it is reasonable to expect that MCPA adsorbs through the same mechanisms.

Table 9 compares the adsorption capacities of the various activated carbons described in the literature towards 2,4-D and MCPA. The TS-AC described herein exhibits satisfactory adsorption capacities comparable to other activated carbons. A more detailed comparison of the different adsorbents can be found in the review papers [3,7,8].

Table 9. Compared to the literature data, the adsorption capacities of 2,4-D and MCPA on activated carbon prepared from tomato stems (TS-AC).

Adsorbent	S _{BET} (m ² /g)	Adsorption Capa	Reference	
Ausorbeit	SBET (III /g)	2,4-D	MCPA	Reference
AC-KOH-550	574	0.840	0.830	This paper
AC-KOH-650 AC-KOH-750	1445 1801	1.417 1.806	1.302 1.721	This paper This paper

Table 9. Cont.

Adsorbent	S (==2/=)	Adsorption Capa	Deference	
Adsorbent	S_{BET} (m ² /g)	2,4-D	MCPA	Reference
AC-NaOH-550	791	0.904	1.056	This paper
AC-NaOH-650	1565	1.637	1.513	This paper
AC-NaOH-750	2087	1.960	1.902	This paper
AC from pistachio shell/CD	556	2.051	1.565	[42]
AC from rice straw/ZnCl ₂	771	1.270	1.640	[48]
AC from rice straw/H ₃ PO ₄	613	1.230	1.640	[48]
AC from particleboard	1211	1.370	1.870	[46]
F-400	800	1.860	1.940	[44]
Sorbo Norit AC	1225	1.490	2.080	[45]
Ceca AC40 AC	1201	1.560	2.599	[45]
AC from PET (K_2CO_3)	1206	1.949	2.450	[49]
AC from willow	1280	2.310	2.413	[47]
AC from hemp shives	1324	2.446	2.460	[47]
AC from miscanthus	1420	2.577	2.677	[47]
AC from flax shives	1587	2.682	2.725	[47]
AC from PAN (KOH)	2828	2.490	2.630	[49]

3.2.3. Effects of Solution pH and Ionic Strength

The adsorption of organic compounds on activated carbon depends on the adsorbate, adsorbent, and solution physicochemical properties. Both the pH of the solution and its ionic strength can influence the dissociation of the adsorbate molecules and the ionization of the adsorbent surface, which can affect adsorption. Depending on the conditions, this can either increase or decrease the efficiency of the adsorption process. Accordingly, a comprehensive understanding of the impact of pH and ionic strength on the adsorption mechanism is indispensable for enhancing the overall process and achieving maximal efficiency in the remediation of these contaminants from aqueous matrices.

Figure 7 demonstrates the strong pH dependence of herbicide adsorption (pH 2.5–10). Both 2,4-D and MCPA were adsorbed most efficiently at the lowest pH (2.5); adsorption decreased drastically with further increases in pH up to about 4. Thereafter, adsorption stabilized at a more or less constant level, and further increases in solution pH from about 4–5 to 10.5 did not result in any noticeable changes in this efficiency. The most drastic changes in adsorption with an increase in solution pH from 2.5 to 10 were observed for AC-KOH-750. In this case, the adsorption efficiency of 2,4-D decreased by more than 57 pp (from 79.4% at pH 2.5 to 22.0% at pH 10), while the MCPA adsorption decreased from 77.5% (pH 2.5) to 16.8% at pH 10. Relatively the least sensitive to pH changes was AC-NaOH-550, for which a decrease in adsorption of 32–33 ppm was observed when the pH of the solution was changed from 2.5 to 10 (from 40% to 7% for 2,4-D and from 41% to 8% for MCPA).

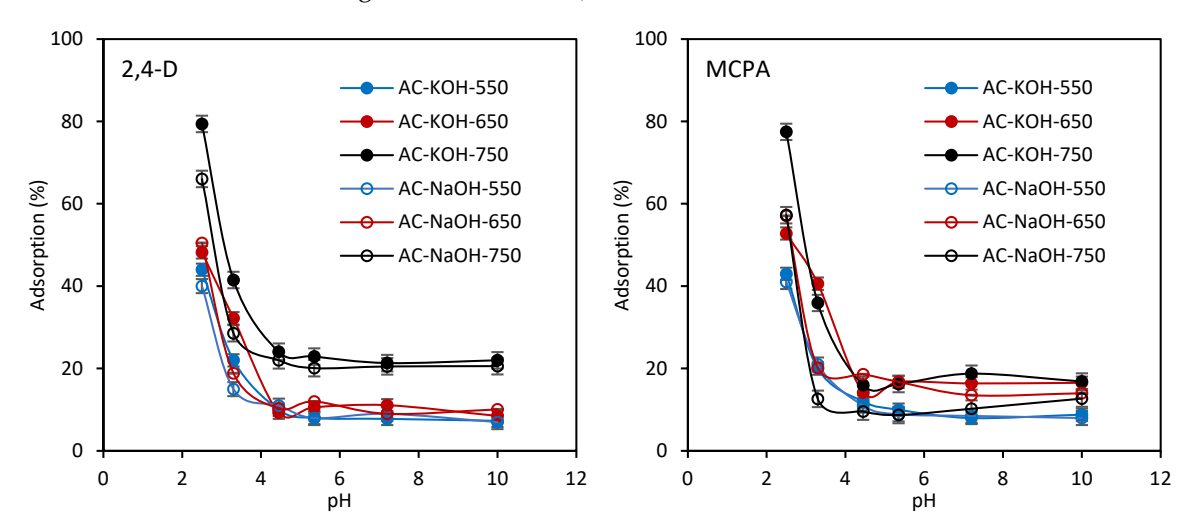


Figure 7. Effect of initial pH on 2,4-D and MCPA adsorption onto activated carbon produced from tomato stems (TS-AC) (experimental conditions: 1 mmol/L herbicide, 0.25 g/L TS-AC, at 23 °C).

The adsorption behavior of 2,4-D and MCPA exhibited high similarity, a predictable outcome given their comparable physicochemical properties (Table 1). In evaluating the influence of pH on adsorption, the acid dissociation constant (pKa) emerges as a critical parameter. The pKa values for 2,4-D and MCPA are 2.98 and 3.14, respectively (Table 1). Consequently, adsorbate molecules are predominantly protonated at pH values below the pKa, while at pH values exceeding the pKa, they exist primarily in anionic form. As the solution pH increases, a progressive dissociation of adsorbate molecules occurs. According to Abdel Daiem et al. [45], at approximately pH 5, 2,4-D molecules in solution are nearly fully ionized. This phenomenon is significant, as the interaction of a neutral molecule with the adsorbent surface differs substantially from that of an ionized molecule. Furthermore, the surface charge of the adsorbent, whether positive or negative, constitutes a pivotal factor in the adsorption process.

The pH_{pzc} values given in Table 2 for the studied activated carbons make it possible to predict how the charge on their surface can change as the pH of the solution is changed. This knowledge can help to explain the regularities observed in Figure 7. The point of zero charge (p H_{pzc}) is the pH at which the adsorbent's surface charge is neutral. The adsorbent surface exhibits a positive charge when pH < pH_{pzc} and a negative charge when $pH > pH_{pzc}$. The pH_{pzc} values for these activated carbons range from 6 to 7 (Table 2). Such close pH_{pzc} values between the different AC explain the similar pH dependence of herbicide adsorption observed on all these activated carbons (Figure 7). Both 2,4-D and MCPA were adsorbed most efficiently at pH 2.5. This suggests that the interaction of the non-dissociated adsorbate molecules (pH below pK_a) with the positively charged adsorbent surface (pH below pH_{pzc}) is most favorable. The observed attenuation of adsorption efficiency under alkaline conditions (pH exceeding both pKa and pH_{pzc}) is plausibly a consequence of repulsive electrostatic forces between phenoxylate anions and the negatively charged surface of the activated carbons. Similar solution pH-dependent adsorption behavior of phenoxy-acetic herbicides has been reported on lignite [50], carbon black, or various activated carbons [44,47,51,52], among others.

The influence of ionic strength on herbicide adsorption onto AC was assessed using data from water and NaCl solutions (0.01, 0.1, and 0.5 mol/L), with the results displayed in Figure 8.

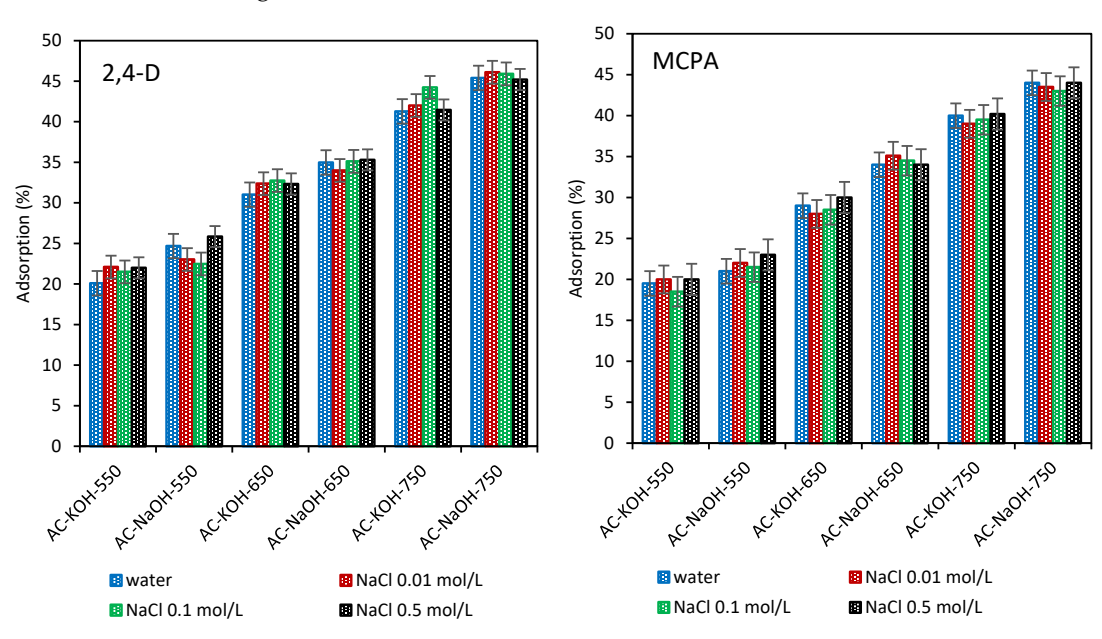


Figure 8. The effect of ionic strength on the adsorption of 2,4-D and MCPA on activated carbon produced from tomato stems (TS-AC) (experimental conditions: 1 mmol/L herbicide, 0.25 g/L TS-AC, original pH, at 23 °C).

Herbicide adsorption remained unaffected by increasing NaCl concentration (Figure 8) across all six activated carbons. Thus, 2,4-D and MCPA adsorption onto tomato stemderived activated carbons is independent of ionic strength. A similar finding (no effect of ionic strength on adsorption) was also observed for the adsorption of 2,4-D and MCPA on various activated carbons [48,53]. On the other hand, a few papers reported enhanced adsorption with increasing concentration of the inorganic salt in solution. This was the case, for example, for the adsorption of 2,4-D on commercial activated carbons [45] or the adsorption of 2,4-D and MCPA on lignite [50]. A slight adsorption decrease in MCPA in the presence of NaCl in solution was also reported [45]. Therefore, it is crucial to recognize that the influence of solution ionic strength on adsorption is system-specific. It depends on the physicochemical properties of both the adsorbate and adsorbent, necessitating individual consideration for each adsorbate—adsorbent system.

3.2.4. Regeneration of the Activated Carbons

The reusability of tomato stem-derived activated carbon (TS-AC) was determined using methanol as a desorbing agent, using three adsorption–regeneration cycles. Figure 9 shows that the TS-AC can be reused thrice with an herbicide removal percentage above 85%.

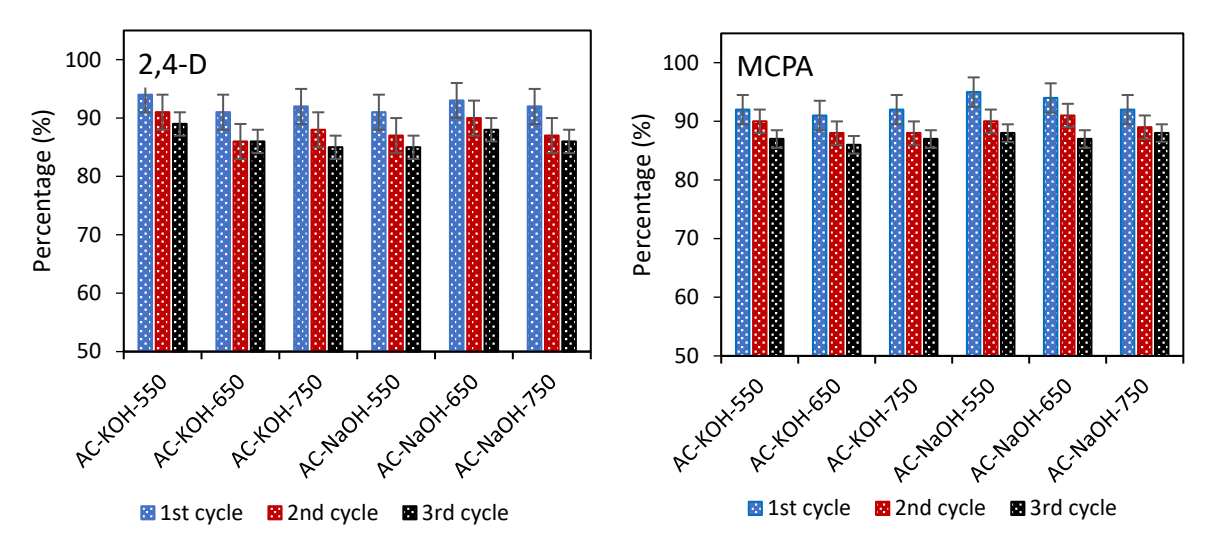


Figure 9. The tomato stem-derived activated carbon (TS-AC) regeneration efficiency using methanol.

The most significant decrease in AC adsorption capacity was observed after the first adsorption–regeneration cycle, averaging 7.8% for 2,4-D and 7.3% for MCPA across all activated carbons. In subsequent cycles, a decrease in herbicide adsorption efficiency by AC was also observed, but the changes were much smaller. After the 2nd adsorption-regeneration cycle, the average adsorption capacity of AC towards 2,4-D and MCPA decreased by 4.0% and 3.3%, respectively, and after the third cycle, by 1.7% and 2.2%, respectively. Moreover, the regeneration efficiency of all six activated carbons tested remained at comparable levels. These results demonstrate that tomato stem-derived AC has good stability and can be reused multiple times without a significant loss of adsorption efficiency.

4. Conclusions

Tomato stem-derived activated carbon (TS-AC) was produced through chemical activation using either potassium hydroxide (KOH) or sodium hydroxide (NaOH) as activating agents, with activation temperatures ranging from 550 to 750 °C. It was observed that an increase in the activation temperature resulted in an enhancement of the BET surface area of the resultant product; furthermore, NaOH was identified as a marginally superior activator.

The produced activated carbons were assessed for their efficacy as adsorbents in the remediation of phenoxyacetic herbicides, including 2,4-dichlorophenoxyacetic acid (2,4-D) and 2-methyl-4-chlorophenoxyacetic acid (MCPA) from aqueous solutions. Adsorption kinetics were analyzed using pseudo-first-order (PFO) and pseudo-second-order (PSO) models, with the PSO model best fitting the experimental data. A strong correlation was observed between the adsorption rate of the herbicides and the mesopore volume of the TS-AC.

Additionally, the adsorption mechanism was investigated using the Weber–Morris (intraparticle diffusion) model, indicating that film diffusion constituted the rate-limiting step in the adsorption process. Subsequently, equilibrium adsorption data were analyzed using the Freundlich and Langmuir isotherms, revealing a superior fit with the Langmuir model. The maximum adsorption capacities of the herbicides exhibited a strong dependence on the porous structure of TS-AC (the micropore volume and the BET surface area). The adsorption of both herbicides was pH-dependent, while ionic strength exhibited no significant effect. Furthermore, regeneration experiments demonstrated that the AC could be reused up to three times, maintaining over 85% herbicide removal with methanol elution. These results demonstrate that agricultural wastes, such as tomato stems, can be successfully valorized through simple activation techniques, with the resultant activated carbons serving as proficient adsorbents for extracting phenoxy herbicides from aqueous environments.

Author Contributions: Conceptualization, K.K., B.D., and A.Ś.; methodology, K.K., B.D., and A.Ś.; formal analysis, M.S.; investigation, K.K., B.D., and A.Ś.; resources, K.K. and B.D.; data curation, B.D.; writing—original draft preparation, K.K., B.D., A.Ś., and M.S.; writing—review and editing, M.S.; visualization, K.K.; supervision, A.Ś.; validation, M.S. All authors have read and agreed to the published version of the manuscript.

Funding: This study received no external funding.

Institutional Review Board Statement: Not applicable.

Informed Consent Statement: Not applicable.

Data Availability Statement: Data are available on request from the authors.

Conflicts of Interest: The authors declare no conflicts of interest.

References

- 1. Wanner, N.; Alcibiade, A.; Tubiello, F.N. Pesticides Use and Trade, 1990–2022. In *FAOSTAT Analytical Briefs*; FAO: Rome, Italy, 2024; p. 13. Available online: https://openknowledge.fao.org/handle/20.500.14283/cd1486en (accessed on 10 May 2025).
- 2. Rani, L.; Thapa, K.; Kanojia, N.; Sharma, N.; Singh, S.; Grewal, A.S.; Srivastav, A.L.; Kaushal, J. An Extensive Review on the Consequences of Chemical Pesticides on Human Health and Environment. *J. Clean. Prod.* **2021**, 283, 124657. [CrossRef]
- 3. Błachnio, M.; Kuśmierek, K.; Świątkowski, A.; Deryło-Marczewska, A. Waste-Based Adsorbents for the Removal of Phenoxyacetic Herbicides from Water: A Comprehensive Review. *Sustainability* **2023**, *15*, 16516. [CrossRef]
- 4. von Stackelberg, K. A Systematic Review of Carcinogenic Outcomes and Potential Mechanisms from Exposure to 2,4-D and MCPA in the Environment. *J. Toxicol.* **2013**, 2013, 371610. [CrossRef]
- 5. Saleh, I.A.; Zouari, N.; Al-Ghouti, M.A. Removal of Pesticides from Water and Wastewater: Chemical, Physical and Biological Treatment Approaches. *Environ. Technol. Innov.* **2020**, *19*, 101026. [CrossRef]
- 6. Ponnuchamy, M.; Kapoor, A.; Senthil Kumar, P.; Vo, D.-V.N.; Balakrishnan, A.; Mariam Jacob, M.; Sivaraman, P. Sustainable Adsorbents for the Removal of Pesticides from Water: A Review. *Environ. Chem. Lett.* **2021**, *19*, 2425–2463. [CrossRef]
- 7. Błachnio, M.; Kuśmierek, K.; Świątkowski, A.; Deryło-Marczewska, A. Adsorption of Phenoxyacetic Herbicides from Water on Carbonaceous and Non-Carbonaceous Adsorbents. *Molecules* **2023**, *28*, 5404. [CrossRef]
- 8. Ighalo, J.O.; Ojukwu, V.E.; Umeh, C.T.; Aniagor, C.O.; Chinyelu, C.E.; Ajala, O.J.; Dulta, K.; Adeola, A.O.; Rangabhashiyam, S. Recent Advances in the Adsorptive Removal of 2,4-Dichlorophenoxyacetic Acid from Water. *J. Water Process Eng.* **2023**, *56*, 104514. [CrossRef]

Appl. Sci. **2025**, 15, 6816 20 of 21

9. Crini, G.; Lichtfouse, E.; Wilson, L.D.; Morin-Crini, N. Conventional and Non-Conventional Adsorbents for Wastewater Treatment. *Environ. Chem. Lett.* **2019**, *17*, 195–213. [CrossRef]

- 10. González-García, P. Activated Carbon from Lignocellulosics Precursors: A Review of the Synthesis Methods, Characterization Techniques and Applications. *Renew. Sustain. Energy Rev.* **2018**, *82*, 1393–1414. [CrossRef]
- 11. Ukanwa, K.; Patchigolla, K.; Sakrabani, R.; Anthony, E.; Mandavgane, S. A Review of Chemicals to Produce Activated Carbon from Agricultural Waste Biomass. *Sustainability* **2019**, *11*, 6204. [CrossRef]
- 12. Zhi, Y.; Shao, J.; Liu, C.; Xiao, Q.; Demir, M.; Al Mesfer, M.K.; Danish, M.; Wang, L.; Hu, X. High-Performance CO₂ Adsorption with P-Doped Porous Carbons from Lotus Petiole Biomass. *Sep. Purif. Technol.* **2025**, *361*, 131253. [CrossRef]
- 13. Bhungthong, S.; Aussawasathien, D.; Hrimchum, K.; Sriphalang, S.-N. Preparation and Properties of Activated Carbon from Palm Shell by Potassium Hydroxide Impregnation: Effects of Processing Parameters. *Chiang Mai J. Sci.* **2018**, 45, 462–473. Available online: https://www.thaiscience.info/Journals/Article/CMJS/10989307.pdf (accessed on 10 May 2025).
- 14. Suhdi; Wang, S.-C. Fine Activated Carbon from Rubber Fruit Shell Prepared by Using ZnCl₂ and KOH Activation. *Appl. Sci.* **2021**, *11*, 3994. [CrossRef]
- 15. Habeeb, O.A.; Kanthasamy, R.; Sethupathib, S.; Yunus, R.M. Optimization and Characterization Study of Preparation Factors of Activated Carbon Derived from Coconut Shell to Remove of H₂S from Wastewater. In Activated Carbon: Prepared from Various Precursors; Ideal International E-Publication Pvt Ltd.: Indore, India, 2017; pp. 44–61, ISBN 978-93-86675-07-1.
- 16. Shao, J.; Wang, Y.; Liu, C.; Xiao, Q.; Demir, M.; Al Mesfer, M.K.; Danish, M.; Wang, L.; Hu, X. Advanced Microporous Carbon Adsorbents for Selective CO₂ Capture: Insights into Heteroatom Doping and Pore Structure Optimization. *J. Anal. Appl. Pyrolysis* **2025**, *186*, 106946. [CrossRef]
- 17. Tiryaki, B.; Yagmur, E.; Banford, A.; Aktas, Z. Comparison of Activated Carbon Produced from Natural Biomass and Equivalent Chemical Compositions. *J. Anal. Appl. Pyrolysis* **2014**, *105*, 276–283. [CrossRef]
- 18. Yagmur, E. Preparation of Low Cost Activated Carbons from Various Biomasses with Microwave Energy. *J. Porous Mater.* **2012**, *19*, 995–1002. [CrossRef]
- 19. Dasgupta, J.; Kumar, A.; Mandal, D.D.; Mandal, T.; Datta, S. Removal of Phenol from Aqueous Solutions Using Adsorbents Derived from Low-Cost Agro-Residues. *Desalin. Water Treat.* **2016**, *57*, 14188–14212. [CrossRef]
- 20. Fu, K.; Yue, Q.; Gao, B.; Wang, Y.; Li, Q. Activated Carbon from Tomato Stem by Chemical Activation with FeCl₂. *Colloids Surf. A Physicochem. Eng. Asp.* **2017**, 529, 842–849. [CrossRef]
- 21. Miziołek, D.; Pytkowska, R.; Serafin, K.; Zaremba, Ł. Production of Agricultural and Horticultural Crops in 2023. In *Statistical Information*; Statistics Poland, Agriculture and Environment Department: Warsaw, Poland, 2024; p. 10. Available online: https://stat.gov.pl/en/topics/agriculture-forestry/agricultural-and-horticultural-crops/production-of-agricultural-and-horticultural-crops-in-2023,2,8.html (accessed on 11 May 2025).
- 22. Boehm, H.P. Surface Oxides on Carbon and Their Analysis: A Critical Assessment. Carbon 2002, 40, 145–149. [CrossRef]
- 23. D1510-24B; Standard Test Method for Carbon Black—Iodine Adsorption Number. ASTM International: West Conshohocken, PA, USA, 2024. [CrossRef]
- 24. D4607-14; Standard Test Method for Determination of Iodine Number of Activated Carbon. ASTM International: West Conshohocken, PA, USA, 2021. [CrossRef]
- 25. Figueiredo, J.L.; Pereira, M.F.R.; Freitas, M.M.A.; Órfão, J.J.M. Modification of the Surface Chemistry of Activated Carbons. *Carbon* **1999**, 37, 1379–1389. [CrossRef]
- 26. Lagergren, S. Zur Theorie Der Sogenannten Adsorption Gelöster Stoffe. *Kungl. Sven. Vetenskapsakad. Handl.* **1898**, 24, 1–39. Available online: https://weburn.kb.se/metadata/824/EOD_2758824.htm (accessed on 11 May 2025).
- 27. Ho, Y.S.; McKay, G. Pseudo-Second Order Model for Sorption Processes. Process Biochem. 1999, 34, 451–465. [CrossRef]
- 28. Ullah, S.; Shah, S.S.A.; Altaf, M.; Hossain, I.; El Sayed, M.E.; Kallel, M.; El-Bahy, Z.M.; Rehman, A.U.; Najam, T.; Nazir, M.A. Activated Carbon Derived from Biomass for Wastewater Treatment: Synthesis, Application and Future Challenges. *J. Anal. Appl. Pyrolysis* 2024, 179, 106480. [CrossRef]
- 29. Nasser, S.M.; Abbas, M.; Trari, M. Understanding the Rate-Limiting Step Adsorption Kinetics onto Biomaterials for Mechanism Adsorption Control. *Prog. React. Kinet. Mech.* **2024**, *49*, 1–26. [CrossRef]
- 30. Morris, J.C.; Weber, W.J. Removal of Biologically Resistant Pollutants from Wastewaters by Adsorption. In *Advances in Water Pollution Research: Proceedings of the International Conference Held in London, September 1962*; Southgate, B.A., Ed.; Pergamon Press: Oxford, UK, 1964; Volume 2, pp. 231–266. [CrossRef]
- 31. Wu, F.-C.; Tseng, R.-L.; Juang, R.-S. Initial Behavior of Intraparticle Diffusion Model Used in the Description of Adsorption Kinetics. *Chem. Eng. J.* **2009**, *153*, 1–8. [CrossRef]
- 32. Langmuir, I. The Adsorption of Gases on Plane Surfaces of Glass, Mica and Platinum. *J. Am. Chem. Soc.* **1918**, *40*, 1361–1403. [CrossRef]
- 33. Freundlich, H. Über Die Adsorption in Lösungen/Over the Adsorption in Solution. Z. Phys. Chem. 1907, 57, 385–470. [CrossRef]

34. Hamdaoui, O.; Naffrechoux, E. Modeling of Adsorption Isotherms of Phenol and Chlorophenols onto Granular Activated Carbon. Part I. Two-Parameter Models and Equations Allowing Determination of Thermodynamic Parameters. *J. Hazard. Mater.* **2007**, 147, 381–394. [CrossRef]

- 35. Gibbs, J.W. A Method of Geometrical Representation of the Thermodynamic Properties of Substances by Means of Surfaces. *Trans. Conn. Acad.* **1873**, 2, 382–404. Available online: https://www3.nd.edu/~powers/ame.20231/gibbs1873b.pdf (accessed on 11 May 2025).
- 36. Zhou, X.; Zhou, X. The Unit Problem in the Thermodynamic Calculation of Adsorption Using the Langmuir Equation. *Chem. Eng. Commun.* **2014**, 201, 1459–1467. [CrossRef]
- 37. Buczek, B.; Biniak, S.; Świątkowski, A. Oxygen Distribution within Oxidised Active Carbon Granules. *Fuel* **1999**, *78*, 1443–1448. [CrossRef]
- 38. Deryło-Marczewska, A.; Świątkowski, A.; Buczek, B.; Biniak, S. Adsorption Equilibria in the Systems: Aqueous Solutions of Organics—Oxidized Activated Carbon Samples Obtained from Different Parts of Granules. *Fuel* **2006**, *85*, 410–417. [CrossRef]
- 39. Kuśmierek, K.; Świątkowski, A.; Skrzypczyńska, K.; Błażewicz, S.; Hryniewicz, J. The Effects of the Thermal Treatment of Activated Carbon on the Phenols Adsorption. *Korean J. Chem. Eng.* **2017**, *34*, 1081–1090. [CrossRef]
- 40. Essandoh, M.; Wolgemuth, D.; Pittman, C.U.; Mohan, D.; Mlsna, T. Phenoxy Herbicide Removal from Aqueous Solutions Using Fast Pyrolysis Switchgrass Biochar. *Chemosphere* **2017**, *174*, 49–57. [CrossRef]
- 41. Deryło-Marczewska, A.; Błachnio, M.; Marczewski, A.W.; Świątkowski, A.; Tarasiuk, B. Adsorption of Selected Herbicides from Aqueous Solutions on Activated Carbon. *J. Therm. Anal. Calorim.* **2010**, *101*, 785–794. [CrossRef]
- 42. Błachnio, M.; Deryło-Marczewska, A.; Charmas, B.; Zienkiewicz-Strzałka, M.; Bogatyrov, V.; Galaburda, M. Activated Carbon from Agricultural Wastes for Adsorption of Organic Pollutants. *Molecules* **2020**, 25, 5105. [CrossRef] [PubMed]
- 43. Nyazi, K.; Baçaoui, A.; Yaacoubi, A.; Darmstadt, H.; Adnot, A.; Roy, C. Influence of Carbon Black Surface Chemistry on the Adsorption of Model Herbicides from Aqueous Solution. *Carbon* **2005**, *43*, 2218–2221. [CrossRef]
- 44. Kim, T.-Y.; Park, S.-S.; Kim, S.-J.; Cho, S.-Y. Separation Characteristics of Some Phenoxy Herbicides from Aqueous Solution. *Adsorption* **2008**, *14*, 611–619. [CrossRef]
- 45. Abdel Daiem, M.M.; Rivera-Utrilla, J.; Sánchez-Polo, M.; Ocampo-Pérez, R. Single, Competitive, and Dynamic Adsorption on Activated Carbon of Compounds Used as Plasticizers and Herbicides. *Sci. Total Environ.* **2015**, *537*, 335–342. [CrossRef]
- 46. Cansado, I.P.P.; Mourão, P.A.M.; Gomes, J.; Almodôvar, V. Adsorption of MCPA, 2,4-D and Diuron onto Activated Carbons from Wood Composites. *Ciência Tecnol. Dos Mater.* **2017**, 29, e224–e228. [CrossRef]
- 47. Doczekalska, B.; Kuśmierek, K.; Świątkowski, A.; Bartkowiak, M. Adsorption of 2,4-Dichlorophenoxyacetic Acid and 4-Chloro-2-Metylphenoxyacetic Acid onto Activated Carbons Derived from Various Lignocellulosic Materials. *J. Environ. Sci. Health Part B* 2018, 53, 290–297. [CrossRef]
- 48. Abdel Daiem, M.M.; Sánchez-Polo, M.; Rashed, A.S.; Kamal, N.; Said, N. Adsorption Mechanism and Modelling of Hydrocarbon Contaminants onto Rice Straw Activated Carbons. *Pol. J. Chem. Technol.* **2019**, *21*, 1–12. [CrossRef]
- 49. da Paixão Cansado, I.P.; Belo, C.R.; Mourão, P.A.M. Pesticides Abatement Using Activated Carbon Produced from a Mixture of Synthetic Polymers by Chemical Activation with KOH and K₂CO₃. *Environ. Nanotechnol. Monit. Manag.* **2019**, *12*, 100261. [CrossRef]
- 50. Kuśmierek, K.; Dąbek, L.; Świątkowski, A. Removal of Phenoxy Herbicides from Aqueous Solutions Using Lignite as a Low-Cost Adsorbent. *Desalin. Water Treat.* **2022**, 260, 111–118. [CrossRef]
- 51. Ocampo-Pérez, R.; Abdel Daiem, M.M.; Rivera-Utrilla, J.; Méndez-Díaz, J.D.; Sánchez-Polo, M. Modeling Adsorption Rate of Organic Micropollutants Present in Landfill Leachates onto Granular Activated Carbon. *J. Colloid Interface Sci.* 2012, 385, 174–182. [CrossRef]
- 52. Doczekalska, B.; Ziemińska, N.; Kuśmierek, K.; Świątkowski, A. Activated Carbons Derived from Different Parts of Corn Plant and Their Ability to Remove Phenoxyacetic Herbicides from Polluted Water. *Sustainability* **2024**, *16*, 7341. [CrossRef]
- 53. Kuśmierek, K.; Białek, A.; Świątkowski, A. Effect of Activated Carbon Surface Chemistry on Adsorption of Phenoxy Carboxylic Acid Herbicides from Aqueous Solutions. *Desalin. Water Treat.* **2020**, *186*, 450–459. [CrossRef]

Disclaimer/Publisher's Note: The statements, opinions and data contained in all publications are solely those of the individual author(s) and contributor(s) and not of MDPI and/or the editor(s). MDPI and/or the editor(s) disclaim responsibility for any injury to people or property resulting from any ideas, methods, instructions or products referred to in the content.